Patient-Specific Mechanical Properties of Diabetic and Healthy Plantar Soft Tissue from Gated MRI

Evan D Williams,[1, 2] Michael J Stebbins,[1,2] Peter R Cavanagh,[2,3] David R Haynor,[4] Baocheng Chu,[4] Michael J Fassbind,[1] Vara Isvilanonda[1, 2] and William R Ledoux,[1, 2, 3]

[1]RR&D Center of Excellence for Limb Loss Prevention and Prosthetic Engineering,
VA Puget Sound, Seattle, WA, USA;

[2]Department of Mechanical Engineering,
[3]Department of Orthopaedics & Sports Medicine,
[4]Department of Radiology
University of Washington, Seattle, WA, USA

Corresponding author:
William R. Ledoux, PhD
ms 151, VA Puget Sound,
1660 S. Columbian Way,
Seattle, WA 98108, USA.
(206) 768-5347 (p)
(206) 764-2127 (f)
Email: wrledoux@uw.edu

Abstract

Foot load rate, load magnitude, and the presence of diseases such as diabetes can all affect the mechanical properties of a person's plantar soft tissue. The hydraulic plantar soft tissue reducer (HyPSTR) is a tool designed to gain insight into which variables are the most significant in determining these properties (namely, stiffness). It can be used with gated magnetic resonance imaging (MRI) to capture three-dimensional images of a foot under dynamic loading conditions. Custom electronics and Labview software simultaneously record system pressure, which is then

translated to applied force values with calibration curves. Data were collected for two subjects, one without diabetes (Subject A) and one with diabetes (Subject B). For a 0.2 Hz loading rate, and strain 0.16 to 0.22, Subject A's heel pad stiffness was 10 N/mm and Subject B's stiffness was 24 N / mm. Maximum test loads were approximately 200 N. Load rate and magnitude limitations (currently both are lower than physiologic values) will continue to be addressed in the next version of the instrument. However, the current HyPSTR did produce a data set for healthy verse diabetic tissue stiffness that agrees with previous findings. In combination with the stiffness data, the MR images are also being used to improve FEA models of the foot as part of a related project.

Keywords

Heel pad, diabetes, MRI-compatible, mechanical properties

Introduction

The mechanical properties of plantar soft tissue affect the foot's ability to distribute loads experienced during normal locomotion. This is especially true for the increasing number of people (9.3% in the U.S.) with diabetes mellitus,[1] but it may also be important among healthy subjects. Research on sub-calcaneal cadaveric samples shows that the modulus of adipose tissue depends on both health (can be twice as high if diabetes is present) and loading rate.[2] When paired with unique anatomy, the difference in plantar soft tissue stiffness causes patient-specific

high stress magnitudes and locations. Recent hypotheses suggest that ulcers, which often lead to amputations, form internally at these points and expand outward to the skin.[3] We designed the Hydraulic Plantar Soft Tissue Reducer (HyPSTR) as a tool to gain understanding of the variables that define high stress in the foot.

The first studies to quantify plantar tissue stiffness measured deformation external to the skin while compressing with a linear or pendulum impact tester.[4-7] These studies lack details of internal foot mechanics, but are very useful for stiffness comparisons if approximating the heel pad as a uniform material. The quality of the data depends on how well the calcaneus is braced against the loading force. If the calcaneus shifts axially, then the deformation of the heel tissue are smaller than reported by an external measuring device.

Ultrasound and fluoroscopy can track the distance between the surface of the skin and the foot's bony structures for living subjects.[8-11] Ultrasound deformation data gives uniaxial information and does not easily differentiate between muscle, fat, and skin tissue types. The major benefits are direct tracking of the calcaneus[8-11] and physiologic kinematics and kinetics,[8, 9, 11] thus producing realistic load magnitudes[12] and rates.

In order to move beyond axisymmetric material properties, MRI has been used to capture three-dimensional (3D) images of feet under various loads.[13-15] Petre et al. have performed a series of static loading tests that represent various phases of the applied force during gait.[14] Their system used a hydraulic apparatus to apply pressure in an MR scanner. Heel tissue stiffness is nonlinear with respect to force as well as loading rate,[2, 9, 16] thus testing these parameters requires adding dynamic loading control to an MRI compatible loading device.

The Hydraulic Plantar Soft Tissue Reducer (HyPSTR) aims to conduct dynamic, in-vivo testing of healthy and diabetic foot tissue, while acquiring 3D deformations with MRI. These data will then be used to determine heel and forefoot moduli with an inverse finite element analysis (FEA).[17] The end result will be a patient specific model that can be used to study the effect of an individual's foot mechanics on internal stresses.

Methods:

Device overview

The design and verification of the HyPSTR has been described previously in detail.[18] It consists of a Labview controlled metal actuator and data acquisition circuit board, paired with a water-filled plastic hydraulic system that is both MRI compatible and capable of applying body weight forces on a subject's foot (Figure 1). Displacement between the actuator and platen is transmitted via vacuum rated tubing. The system uses gated MR image acquisition to record 3D deformations of internal foot tissue while under dynamic, cyclic loading from the platen. Generally, gated MRI is used for imaging lung, heart, or other circulatory anatomy and each image capture sequence is triggered from the subject's monitored heart pulse. In order to increase control over imaging rates and to synchronize them with the HyPSTR's loading period, we used Labview to generate a peripheral pulse unit signal (PPU) that travels via fiber optic cable to the MR instrumentation. The ultimate goal was to record several complete image volumes of a foot at various loading and unloading states. Gated MRI records a small snapshot of the 3D space during each pass of the system. After approximately 20 min of imaging cycles, the data are stitched together to complete the image at each loading phase (Figure 2). The HyPSTR was also

designed to accept a platen fitted with an ultrasound probe for preliminary testing before carrying out more extensive MRI tests.

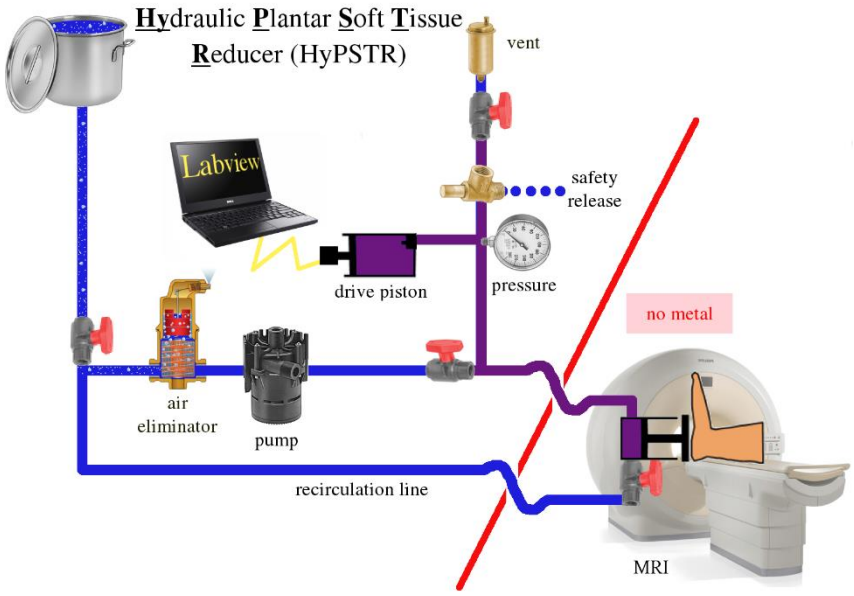

Figure 1. Instrument schematic showing fill and recirculation lines in blue and high pressure hydraulic lines in purple. Valves were closed to isolate the purple lines prior to testing.

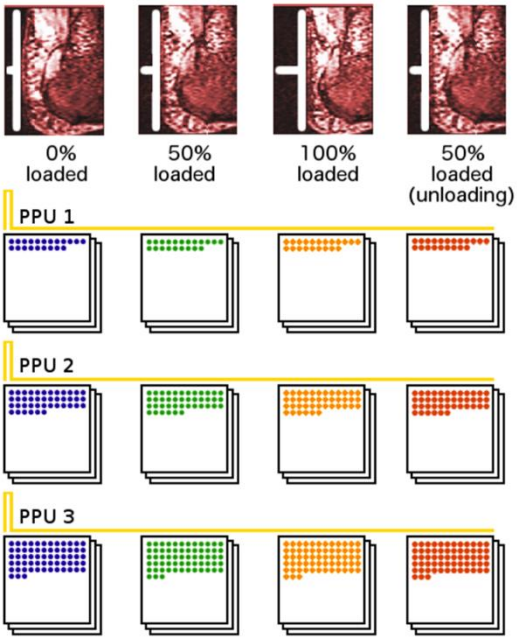

Figure 2. Gated MRI schematic showing 4 phase acquisitions for 3 cycles. The HyPSTR will collect approximately 16 phases over 270 cycles during subject trials.

Protocol

Two subjects were enrolled in this study, which was approved by the VA Puget Sound Health Care System IRB. Subject A had no history of diabetes and was 93 kg in mass, 180 cm tall, and 43 years old. Subject B had Type II diabetes and was 70 kg in mass, 170 cm tall, and 31 years old.

Regardless of the imaging technology (ultrasound or MR), the pre-test protocol was the same. The HyPSTR's hydraulic tubing was filled and air bubbles were removed from the system with a recirculation pump connected to a hydronic air eliminator (VJR075TM; Spirotherm, Glendale Heights, IL). The subject laid horizontally on a backboard on a table that was large enough to also accommodate the hydraulic system. The loading platen and backboard were secured relative to each other with polycarbonate rails and a set of plastic clamps (Figure 3). The

right foot and lower leg were held tightly by a custom ankle foot orthotic (AFO) that was also fastened to the jig. Shoulder and chest straps were used to provide additional contact points to counteract skeletal movement from the platen pushing on the calcaneus. The platen position was adjustable, and the AFO was replaceable, to allow for either hind foot or forefoot testing and different size legs.

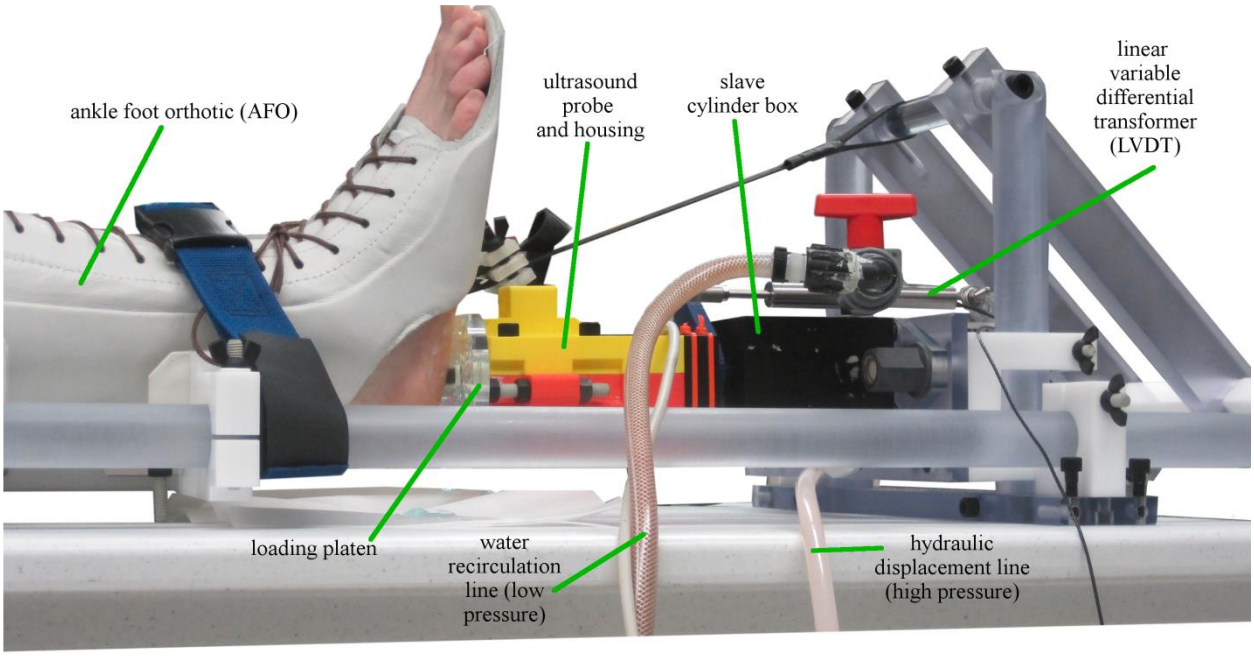

Figure 3. Subject's leg and foot was secured by the (white) ankle-foot orthosis that is attached to polycarbonate rails. The slave cylinder (black) is in series with an ultrasound probe held in plastic (yellow and red) and with a polycarbonate platen. Note the ultrasound probe was used to validate the system and it was removed before any MRI scanning was conducted.

Ultrasound testing provided a means of checking protocols and making fit adjustments to the jig before going to the MRI facility. Because there were no metal restrictions in the lab (as opposed to in the MR core), a Linear Variable Differential Transformer (LVDT) was attached to track the platen position (Figure 3). Thus, platen displacement could be compared to foot tissue deformation in order to quantify any calcaneus movement due to loading (Figure 4). Some

amount of skeletal shift was acceptable as long as it was repeatable. If calcaneal motion was not repeatable, this would lead to image blur in the gated MRI acquisitions.

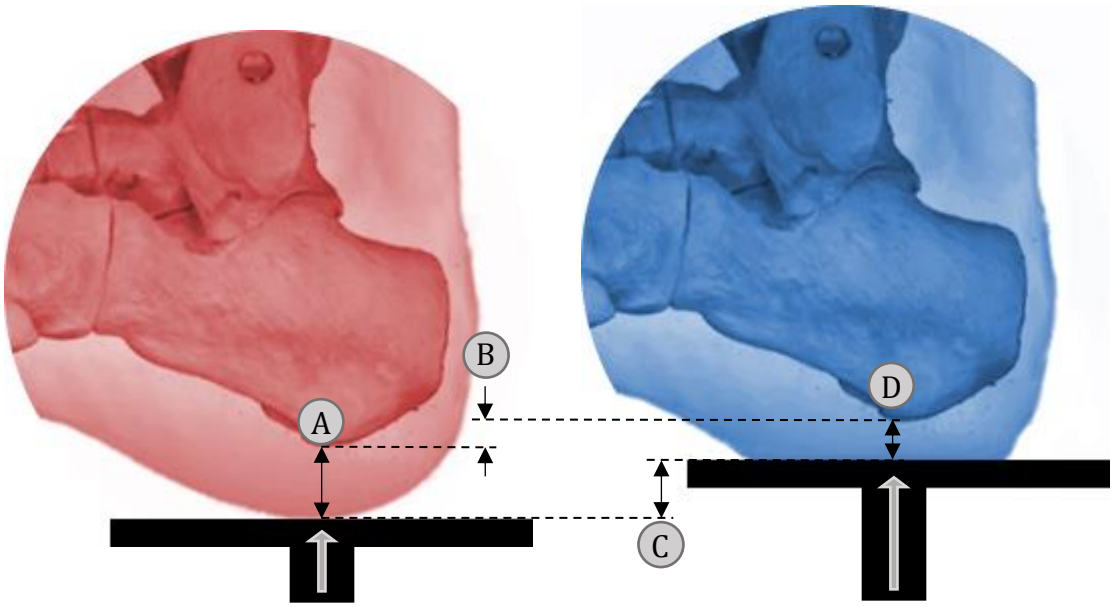

A = unloaded fat pad thickness B = calcaneus shift C = platen movement D = loaded fat pad thickness

Figure 4. Even if the subject's leg is well secured, his/her skeletal structure will slide in the same direction as the platen load. The left (red) foot shows the unloaded state. The right (blue) foot shows the maximally loaded state. B = C + D – A.

Ultrasound test parameters (i.e., displacement of 19 mm and 270 cycles) were set to match those expected during subsequent MRI scans. The subject's mass and a pre-defined pressure-force calibration curve[18] were used to approximate the amount of hydraulic pressure needed to reach the desired loading, ideally 50% to 100% bodyweight. A second calibration curve, the

displacement between the master cylinder and slave platen, was determined along with the corresponding pressure. Because of the calcaneal shift, the required motor displacement was generally higher than calculated from the calibration curves, which were determined with a rigid backstop and a silicone block.[18] The loading platen was advanced to make visual contact with the subject's foot and then cycled ten times to precondition the plantar tissue. Previous HyPSTR verification tests showed a pressure ringing, or water hammer, problem with platen speeds greater than 0.2 Hz.[18] A stable pressure signal was needed to calculate the applied force on the platen, thus all tests were completed with 0.2 Hz cycles even though the motor was capable of a 6 Hz rate for the given piston travel.

For MRI tests the same protocol was followed with the addition imaging synchronization via PPU timing control. Platen position was tracked with four fiduciary markers set into holes machined in the back of the MRI-specific loading platen (Figure 5). The heel pad thickness was reported as the distance between the platen and inferiormost point of the calcaneus. Rates and magnitudes of the sine wave loading profile were kept as similar as possible for each respective subject between the two types of imaging. Small variations in rate (+/- $2x10^{-4}$ Hz) and displacement occurred because of the impossibility of securing a subject in the HyPSTR in precisely the same manner on different days. The AFO and chest harness system relies primarily on friction to resist skeletal shifting. It was not geometrically possible to have a subject bend his/her knee (a common backstop used in other foot stiffness studies) and still fit into the narrow MR core.

Precise synchronization between the MR and Labview VI was necessary to match force values to deformations. For example, if the PPU was late arriving to the MR controls, a particular deformation would correspond to an earlier force reading, or vice versa. Elsewhere, we

have discussed the sources and solutions for all identifiable timing inconsistencies.[18,19] For the scope of this study, it is sufficient to know that timing errors were minimized through careful procedures and real-time displacement feedback during the imaging and then accounted for with custom functions in MatLab post-processing.

For the ultrasound and MR data, an average, representative five second (0.2 Hz) loading curve was calculated from 260 platen cycles (270 minus 10 preconditioning). Gated MR images, and thus the skin, fat, and muscle tissue deformations, were aligned with the loading curve by obtaining each phase's timestamp from image header files (Figure 5). These acquisitions were centered on each time stamp, but not instantaneous. Thus, the force for each phase was averaged over the 152 ms acquisition window.

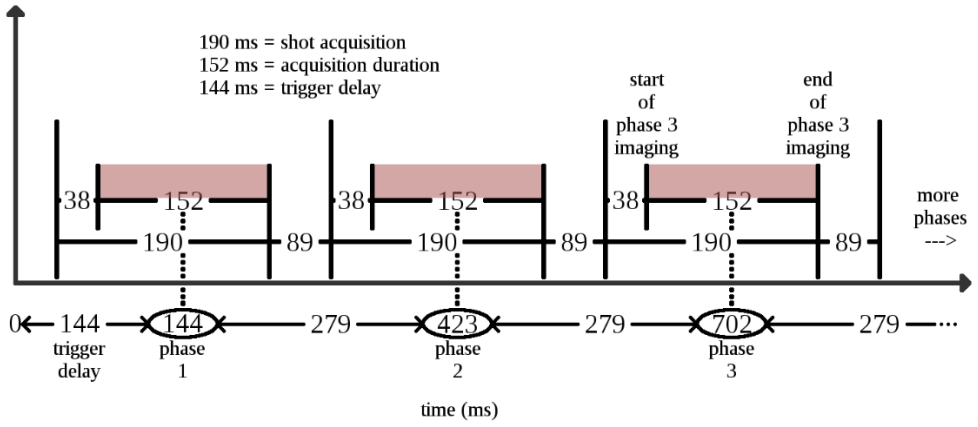

Figure 5. Timing schematic of the window of data acquisition surrounding each phase's time stamp.

Results

Skeletal shifting (Figure 6) tracked during the ultrasound tests was 12.65 ± 0.07 mm (mean ± standard deviation) for Subject A and 12.45 ± 0.04 mm for Subject B. The 0.2 Hz target frequency was matched closely at 0.1998 ± 0.0008 Hz.

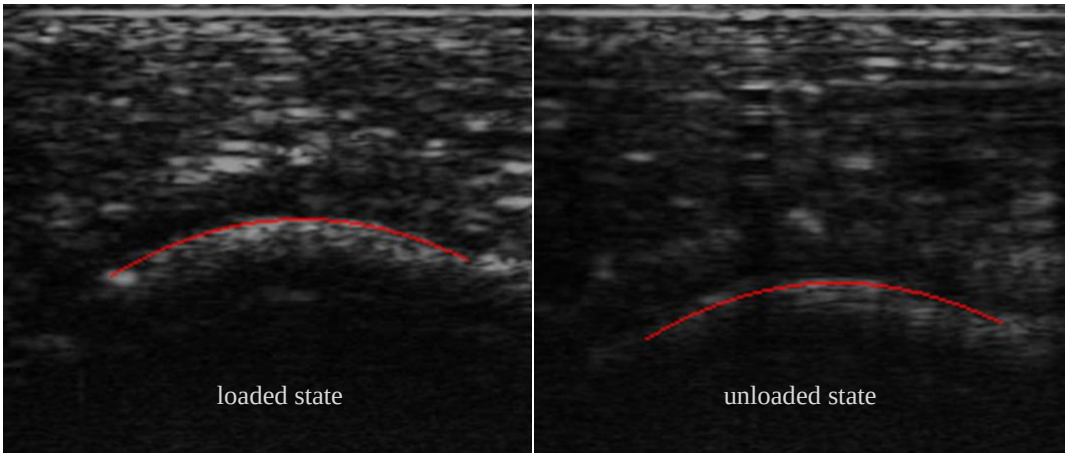

Figure 6. Tracking the calcaneus position with in-house Matlab software during ultrasound tests.

Sixteen MR image volumes were captured for both Subject A and B (Figure 7). Plantar tissue forces were analyzed with respect to time (Figure 8) and deformation (Figure 9). The peak force for Subject A was 216.0N at 30% strain (5.69 mm deformation). The peak force for Subject B was 179.6N at 21% strain (4.00 mm deformation). Linear approximations (Table 1) show that the heel pad stiffness was between 1.73 and 3.64 times stiffer for Subject B near the peak deformation.

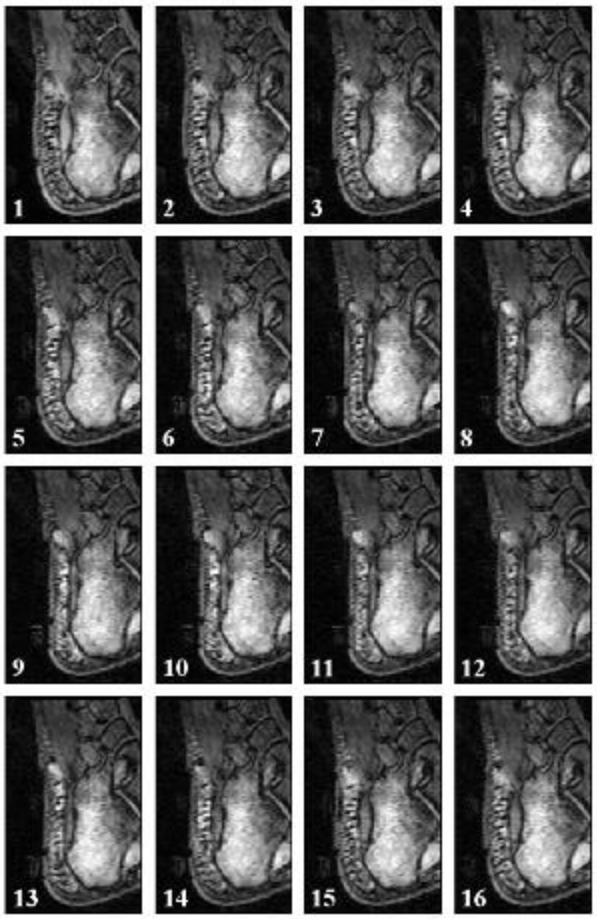

Figure 7. Center image slice of each gated MRI phase for Subject B.

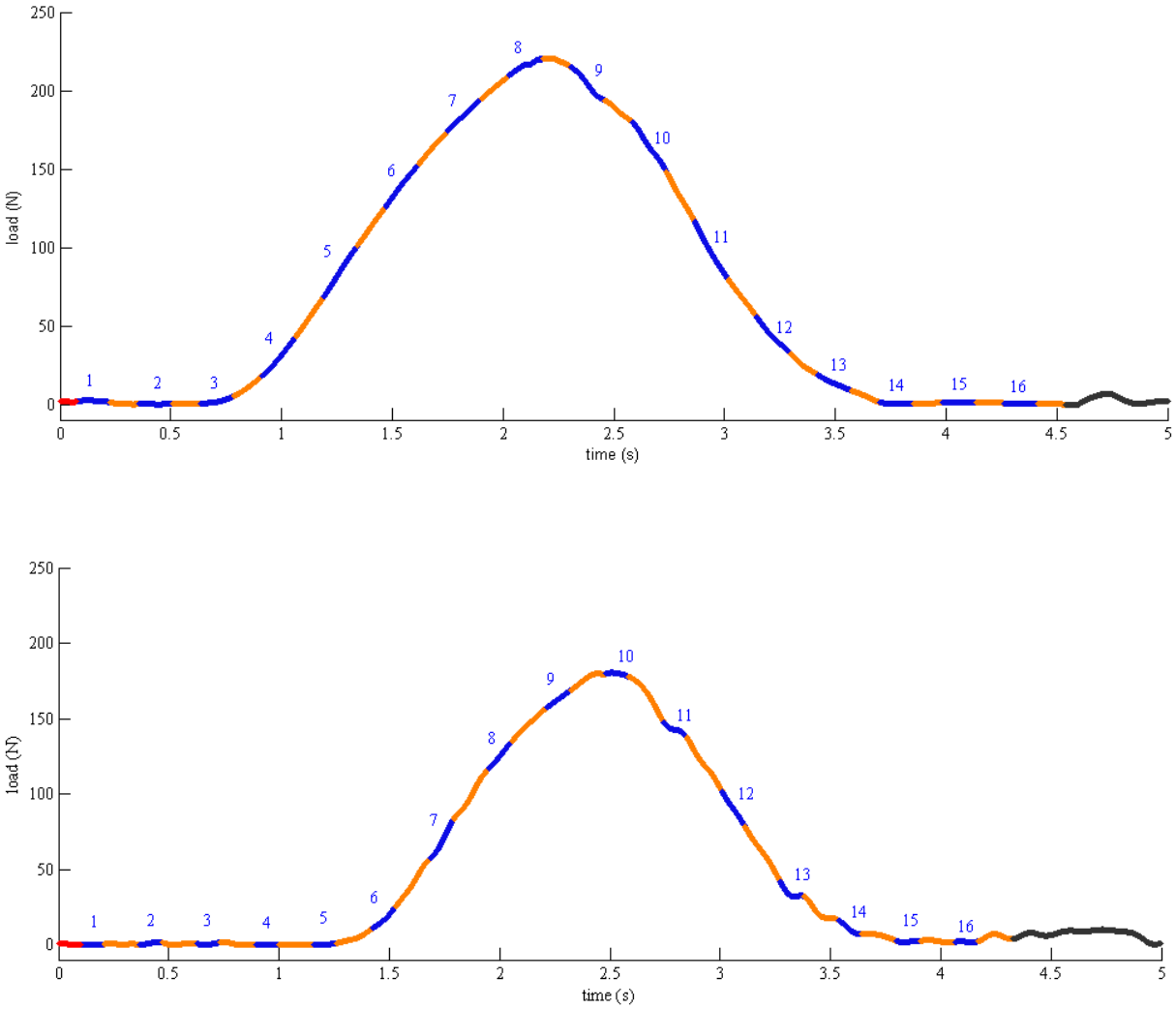

Figure 8. Subject A (top) and Subject B (bottom) load phases during gated MRI acquisition. Red, orange, and black segments represent times that the MR hardware is not recording image data. Blue segments (152ms in duration) are the acquisition windows.

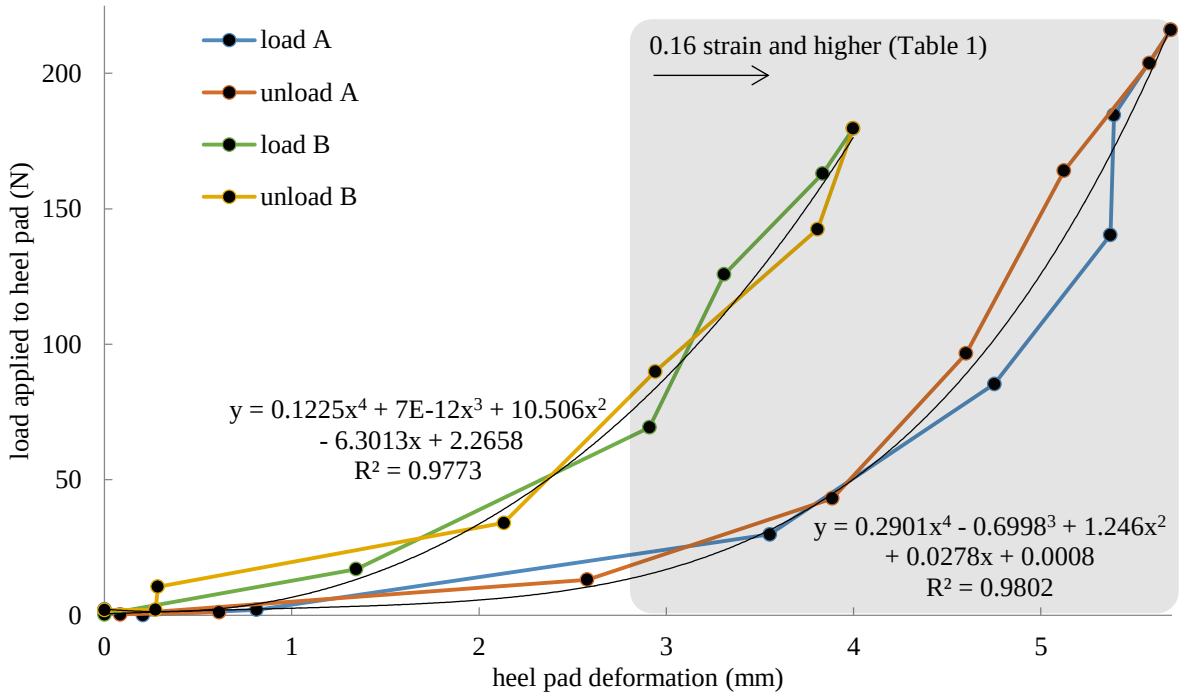

Figure 9. Load vs. deformation curve for Subject A (top) and Subject B (bottom) and 4th order polynomial regressions fit to the data.

Table 1. Heel pad deformation, force, and stiffness for 0.16 strain and higher, calculated from the derivative of the regressions in Figure 9. The maximum strain for Subject B was 0.22. The maximum strain for Subject A was 0.30.

Strain	Deformation		Force		Stiffness (tangent)		Relative stiffness
	Subj. A	Subj. B	Subj. A	Subj. B	Subj. A	Subj. B	Subj. B / Subj. A
(mm/mm)	(mm)	(mm)	(N)	(N)	(N/mm)	(N/mm)	(N/mm) / (N/mm)
0.16	3.02	2.99	16.22	87.16	20.29	69.63	3.43
0.18	3.39	3.36	25.55	115.66	29.65	83.04	2.80
0.20	3.77	3.74	38.92	149.42	41.78	97.83	2.34
0.22	4.15	4.11	57.43	188.99	57.03	114.16	2.00
0.24	4.52	-	82.35	-	75.80	-	-
0.26	4.90	-	115.06	-	98.44	-	-
0.28	5.28	-	157.09	-	125.34	-	-
0.30	5.66	-	210.12	-	156.87	-	-

Discussion

The HyPSTR was designed as a tool to investigate the 3D material properties of plantar soft tissue in diabetic and healthy subjects, with respect to loading rate/magnitude and tissue type. This is particularly relevant to the growing population of people with diabetes[1] who are at risk of developing foot ulcers that can lead to limb amputation. While there were some limitations in the testable range of loading magnitudes and rates, the instrumentation made significant progress toward achieving dynamic, *in vivo*, and patient-specific material property analysis. Furthermore, the data agreed with previous findings that diabetic tissue is stiffer than healthy tissue[2] and the results were used as inputs (volumetric images) and benchmarks (force vs deformation curves) for FEA models.[17]

Calcaneus tracking with an ultrasound probe showed that subjects' skeletal shifts were repeatable along the loading axis with standard deviations less than 0.1 mm. The magnitude of the shift was approximately 12.5 mm. The AFO prevented all motion between the skin and the loading jig, but shear between the skin and bone was not preventable. To compensate for this skeletal shift, the platen was moved farther than the original displacement target, which did not seem to affect the precision of system displacement and load magnitude.

The MRI load vs deformation curves (Figure 9) showed that Subject B had stiffer tissue than Subject A for comparable strains (Table 1). Pai and Ledoux report that the modulus of cadaver adipose tissue with diabetes is 1.93 times greater than that of healthy tissue. The HyPSTR stiffness values for Subject B (diabetes) were 2.65 times stiffer at 0.2 Hz (average for 16% to 22% strain). To determine an estimate for modulus, we used the MRI data to measure Subject A and B initial heel pad thicknesses, 18.85 mm and 18.69 mm, and loaded platen contact areas

3850 mm^2 and 3888 mm^2, respectively. The values, 67 kPa (Subject A) and 115 kPa (Subject B), show the same trend as the stiffness data (Subject B was greater than Subject A).

A pendulum impact *in vivo* materials study by Aerts and De Clercq found that heel pad stiffness varied between 50 and 150 N/mm for the loading rate range 370 to 960 mm/s.[4] The initial heel pad thickness was not measured, thus the strains are not known, but loading was large enough to reach a mostly linear region on the stiffness plot. The HyPSTR data set had smaller maximum loads (approximately 200 N vs 200 to 1000 N), a slower loading rate (8 mm/s), and a different strategy for securing the lower leg (calcaneal shift was minimized and then accounted for with bone tracking in the MR images vs mechanical grounding of a bent knee). These differences make a direct comparison difficult, but HyPSTR stiffness values (Table 1) are within the range reported by Aerts and De Clercq. To approximate the stiffness in the same linear region, the last 1 mm of deformation for Subject A and Subject B has a stiffness of 71 N/mm (0.24 to 0.30 strain) and 91 N/mm (0.16 to 0.22 strain), respectively.

Limitations for this study include foot loading rates and magnitudes that were smaller than physiological levels[12] and MRI image resolution restrictions due to the control computer hardware. The rate limit, due to pressure ringing in the hydraulic column, might be solvable by using narrower tubing, a pressure snubber, or more compressible hydraulic fluids such as glycol mixtures or oil. Load magnitudes higher than approximately 200 N were uncomfortable to the dorsal surface of test subjects' feet in the AFO brace over sustained (20 min) cycling. Image resolution in the MRI data was courser than expected. The MR software was capable of selecting higher quality parameters, but would have required more computer RAM/processing capacity. The 1 mm x 1 mm x 1 mm voxel (3D pixel) was not sufficient to differentiate between skin and fat tissue deformations. If fewer gated phases are acquired, perhaps by removing some that are

unloaded at the start and end of the load cycle (Figure 8), more computational resources will be available for image quality. There may be a more optimal balance between scan duration (subject compliance/cost), number of gated phases, voxel resolution, and total image volume.

The HyPSTR has successfully collected data that can be used to improve our understanding of stress distribution in the foot. Its primary value is being able to capture dynamic (though currently with limitations) material behavior simultaneously with patient-specific internal and external anatomy. The force and 3D deformation data set gives a complete mechanical representation of the foot for use in inverse FEA modeling projects.[17] Future versions of the HyPSTR will follow the same conceptual goals, while improving the range of the load magnitude/rate and image resolution variables.

Acknowledgments

This work was supported by VA RR&D Grant A6973R.

Greg Wilson PhD, UW – for help with determining gated MRI timing schematics and important dynamic scanning variables.

John Shaffer – for design consultation and construction of the ankle-foot orthotics at American Artificial Limb, Seattle, WA.

References

1. National diabetes fact sheet, 2014. *Centers for Disease Control and Prevention* 2014.
2. Pai S, Ledoux WR. The compressive mechanical properties of diabetic and non-diabetic plantar soft tissue. *Journal of biomechanics*. 2010; 43: 1754-60.
3. Gefen A. Plantar soft tissue loading under the medial metatarsals in the standing diabetic foot. *Medical engineering & physics*. 2003; 25: 491-9.
4. Aerts P, De Clercq D. Deformation characteristics of the heel region of the shod foot during a simulated heel strike: the effect of varying midsole hardness. *J Sports Sci*. 1993; 11: 449-61.

5. Kinoshita H, Ogawa T, Kuzuhara K, Ikuta K. In vivo examination of the dynamic properties of the human heel pad. *Int J Sports Med*. 1993; 14: 312-9.
6. Robbins SE, Gouw GJ, Hanna AM. Running-related injury prevention through innate impact-moderating behavior. *Medicine and science in sports and exercise*. 1989; 21: 130-9.
7. Valiant GA. An in vivo determination of the mechanical characteristics of the human heel pad. 1985.
8. Cavanagh PR. Plantar soft tissue thickness during ground contact in walking. *Journal of biomechanics*. 1999; 32: 623-8.
9. De Clercq D, Aerts P, Kunnen M. The mechanical characteristics of the human heel pad during foot strike in running: An in vivo cineradiographic study. *Journal of biomechanics*. 1994; 27: 1213-22.
10. Erdemir A, Viveiros ML, Ulbrecht JS, Cavanagh PR. An inverse finite-element model of heel-pad indentation. *Journal of biomechanics*. 2006; 39: 1279-86.
11. Gefen A, Megido-Ravid M, Itzchak Y. In vivo biomechanical behavior of the human heel pad during the stance phase of gait. *Journal of biomechanics*. 2001; 34: 1661-5.
12. Chin Teoh J, Bena Lim Y, Lee T. Minimum indentation depth for characterization of 2nd sub-metatarsal head and heel pad tissue properties. *Journal of biomechanics*.
13. Gefen A, Megido-Ravid M, Azariah M, Itzchak Y, Arcan M. Integration of plantar soft tissue stiffness measurements in routine MRI of the diabetic foot. *Clinical biomechanics*. 2001; 16: 921-5.
14. Petre M, Erdemir A, Cavanagh PR. An MRI-compatible foot-loading device for assessment of internal tissue deformation. *Journal of biomechanics*. 2008; 41: 470-4.
15. Weaver JB, Doyley M, Cheung Y, et al. Imaging the shear modulus of the heel fat pads. *Clinical biomechanics*. 2005; 20: 312-9.
16. Ledoux WR, Blevins JJ. The compressive material properties of the plantar soft tissue. *Journal of biomechanics*. 2007; 40: 2975-81.
17. Isvilanonda V. Finite Element Modeling of the Foot. *University of Washington*. 2015; Mechanical Engineering Department.
18. Williams ED, Ledoux WR, Cavanagh PR. Design and Verification of a Gated MRI Technique to Determine Mechanical Properties of Plantar Soft Tissue. 2015.
19. Williams ED. Hydraulic Plantar Soft Tissue Reducer - structural properties of the human heel pad. *University of Washington*. 2015; Mechanical Engineering Department.